sustainability

Article

Evaluation and Analysis of CFI Schemes with Different Length of Displaced Left-Turn Lanes with Entropy Method

Binghong Pan [1,*], Shasha Luo [1], Jinfeng Ying [1], Yang Shao [2], Shangru Liu [1], Xiang Li [1] and Jiaqi Lei [1]

[1] Room504, JiaoTong Building, Highway School, Chang'an University, 2nd South Ring Road, Xi'an 710064, China; 2019121224@chd.edu.cn (S.L.); 2019121237@chd.edu.cn (J.Y.); 2019221214@chd.edu.cn (S.L.); 2019121223@chd.edu.cn (X.L.); 2019121236@chd.edu.cn (J.L.)

[2] Institute of Posts, School of Modern Posts (Logistics School), Xi'an University of Posts & Telecommunications, Xi'an 710061, China; shaoyang2020@xupt.edu.cn

* Correspondence: panbh@chd.edu.cn

Abstract: As an unconventional design to alleviate the conflict between left-turn and through vehicles, Continuous Flow Intersection (CFI) has obvious advantages in improving the sustainability of roadway. So far, the design manuals and guidelines for CFI are not enough sufficient, especially for the displaced left-turn lane length of CFI. And the results of existing research studies are not operational, making it difficult to put CFI into application. To address this issue, this paper presents a methodological procedure for determination and evaluation of displaced left-turn lane length based on the entropy method considering multiple performance measures for sustainable transportation, including traffic efficiency index, environment effect index and fuel consumption. VISSIM and the surrogate safety assessment model (SSAM) were used to simulate the operational and safety performance of CFI. The multi-attribute decision-making method (MADM) based on an entropy method was adopted to determine the suitability of the CFI schemes under different traffic demand patterns. Finally, the procedure was applied to a typical congested intersection of the arterial road with heavy traffic volume and high left-turn ratio in Xi'an, China, the results showed the methodological procedure is reasonable and practical. According to the results, for the studied intersection, when the Volume-to-Capacity ratio (V/C) in the westbound and eastbound lanes is less than 0.5, the length of the displaced left-turn lanes can be selected in the range of 80 to 170 m. Otherwise, other solutions should be considered to improve the traffic efficiency. The simulation results of the case showed CFI can significantly improve the traffic efficiency. In the best case, compared with the conventional intersection, the number of vehicles increases by 13%, delay, travel time, number of stops, CO emission, and fuel consumption decrease by 41%, 29%, 25%, 17%, and 17%, respectively.

Keywords: CFI; displaced left-turn lanes length; VISSIM; SSAM; sustainable transportation; MADM; entropy method

check for updates

Citation: Pan, B.; Luo, S.; Ying, J.; Shao, Y.; Liu, S.; Li, X.; Lei, J. Evaluation and Analysis of CFI Schemes with Different Length of Displaced Left-Turn Lanes with Entropy Method. *Sustainability* **2021**, *13*, 6917. https://doi.org/10.3390/su13126917

Academic Editors: Andrew Shing-Tao Chang and Chaohui Wang

Received: 8 May 2021
Accepted: 12 June 2021
Published: 19 June 2021

1. Introduction

The rapid growth of the number of motor vehicles has brought about serious traffic congestion. The time costs due to delays, the additional economic costs, and the environmental pollution costs caused by urban traffic congestion seriously affect public life and restrict economic development [1,2]. Under this circumstance, sustainable roadways and sustainable transportation, which aim at solving traffic congestion, reducing environmental pollution and optimizing resource utilization, should be vigorously developed, which is of great significance to the urban development and transportation.

An intersection is a bottleneck node in an urban road network [3]. Solving the congestion of intersections is the key to settling down the problem of urban traffic congestion, while the conflict between left-turn and through vehicles is the key factor in increasing vehicles' delay and reducing vehicle throughput of intersections [4–6]. Setting a left-turn protection phase could alleviate the conflict between left-turn vehicles and through vehicles, but it will increase delay. The solutions to these problems have always been issues that engineers have devoted themselves to solve. In terms of the algorithm of the traffic signal control, an SFM (Semi-decentralized Feudal Multi-agent)-LSAC (Learned-goal Soft Actor-Critic) algorithm was proposed for multi-intersection traffic signal control [7]. Another article developed a novel traffic coordination control method to optimize the coordination parameters of green time plans and offset for all intersections along oversaturated arterial [8]. Besides, considering the settings of left-turn bays, two single-objective optimization models were developed for paired intersections with uncoordinated and coordinated signals [9]. A review article analyzed the current method of traffic signal timing and presented several directions for future research [10]. An unconventional left-turn waiting area design is also an innovative approach to mitigate traffic congestion at signalized intersections. Some scholars evaluated the effects of left-turn waiting areas and exclusive left-turn lanes on capacity and level of service at signalized intersections [11,12]. Another scholar proposed a series of design pattern left-turn waiting areas for different combinations of spatial and temporal treatments of left-turn movements [13]. In addition, a procedure for evaluating the impacts of left-turn waiting areas at signalized intersections considering multiple performance measures was presented, and the implementation of left-turn waiting areas on both approaches with a dual-lagging left-turn phase was recommended [14]. A previous study showed the utilization of the left-turn waiting area significantly improves the discharge rate of the through lane without compromising the efficiency of left-turning flows [15]. Another paper proposed a dynamic strategy on the prohibition of left turns [16]. In terms of optimizing traffic control strategies, a paper used a mathematical model for a traffic equilibrium network to solve the problem of how to select the most appropriate combination of these strategies in the network [17]. Signalization and channelization design is also a method to reduce traffic deceleration, delay, and other problems at intersections [18]. And an exclusive spur dike U-turn lane design (ESUL) can be used to solve the traffic congestion and conflicts in the U-turn diversions and merge segments [19].

With the increase in traffic demand, the effects of the above strategies have reached theoretical limits. Traffic engineers have begun to seek new geometric designs to improve operation efficiency for urban intersections; thus, the unconventional intersection design emerges.

1.1. Unconventional Intersections

A contraflow left-turn lane (CLL),one of unconventional intersections, provides additional left-turn capacity at intersections by dynamically using contraflow exit lanes [20–23]. As another unconventional intersection, the U-turn (UT) requires left turning vehicles to follow through vehicles crossing the intersection and U-turn at the downstream opening to achieve indirect left turning [24,25]. The UT design reduces the number of phases but increases the travel time of left-turn vehicles. A parallel flow intersection (PFI) is a kind of displaced left-turn lane, which releases the through traffic flow of one road and the left-turn traffic flow of another road simultaneously [26]. The disadvantage of the PFI is that left-turn vehicles could encounter three signal lights. An upstream signalized crossover intersection (USC) eliminates the conflict between left-turn vehicles and through vehicles by allowing left turning vehicles and through vehicles to cross to the left side of the road upstream of the main intersection, while right turning vehicles remain on the right side [27]. In addition, an innovative design of roundabouts has been proposed, and some scholars have evaluated its effect on the reduction of road pollutant emissions [28,29]. The intersection with special width approach lanes is also an unconventional intersection [30].

1.2. Continuous Flow Intersection

Several unconventional intersections are described above. However, the most widely recognized and used is the continuous flow intersection (CFI) (also named a displaced left-turn intersection, DLT). A CFI redistributes the rights to use the lanes by setting a crossover intersection and pre-signal at a distance upstream of the main intersection, and guides the left-turn vehicles at the crossover intersection to the outside of the opposite through vehicles (the displaced left-turn lane); finally, the left-turn vehicles are released together with the through vehicles [31]. In this way, the conflict between left-turn vehicles and the opposite through vehicles is advanced to the crossover intersection, and the vehicles at the intersections can operate under a two-phase signal [32]. The CFI design includes two types: full CFI and two-leg CFI. For a full CFI design, the main intersection is located in the center, and the four crossover intersections are located in the four approaching legs [32]. A two-leg CFI is an intersection containing displaced left-turn legs in two directions, with the other two legs having the same geometry as a conventional intersection [31]. The CFI design not only makes full use of the idle road resources at intersections but also has obvious advantages in reducing the number of signal phases, reducing the environmental pollution, shortening the cycle time, and improving the capacity, so that it can be considered as a sustainable intersection design. Recently, the CFI has attracted an increasing amount of attention, and a great amount of research has been carried out, focusing on the geometric layout, traffic signal control, and traffic efficiency.

1.2.1. Geometric Layout of CFI

The geometric layout of CFI has always been one of the focuses of scholars' research, which may be attributed to the improvement of CFI capacity and its unique geometric layout. So far, scholars have done a lot of research studies. A study developed a set of planning-stage models for the geometry of the CFI design [31]. The geometry physical model and design principles of the CFI were illustrated in another study [33]. An improved CFI layout was proposed to ensure the safety of pedestrians and non-motor vehicles and to eliminate the conflict between left-turn and right-turn vehicles [34]. Some scholars optimized the design of the intersection, the lane marking, and the length of the displaced left-turn lane by formulating mixed integer nonlinear programming [35]. VISSIM micro simulation was used to discuss the distance between the main intersection and the crossover intersection under different traffic conditions. The results showed that the larger the traffic volume is, the more distance between the main intersection and the crossover intersection is needed [36]. A study showed that the length between the main intersection and the crossover is the most important design variable affecting the operation effect of a CFI [37]. There are also papers arguing that the delay of a CFI is not only related to the traffic volume but also the length of the shifted left-turn lane, and its length was determined by identifying the queue hysteresis position [32]. A guide for the displayed left-turn intersection published by the Federal Highway Administration points out that the distance between a main intersection and a pre intersection is generally between 100 and 150 m, but it is not always possible to stay within these ranges [38]. In previous studies, the length of the displaced left-turn lane was 100 m [39]. A simplified CFI without a sub-intersection, called CFI-Lite, was proposed to solve the problem in which the geometric conditions of some intersections do not meet the requirements of setting left-turn waiting areas at sub-intersections [40]. In addition, relevant papers have also studied the design scheme of pedestrian crossing facilities at CFIs [39]. The innovative design of a left-turn bicycle at a CFI has been put forward, which can eliminate the conflict between left-turn bicycles and opposite through vehicles [3]. In addition, a geometric improvement to the CFI was analyzed to enhance pedestrian accommodations [41].

1.2.2. Signal Control of CFI

Due to the uniqueness of the geometric layout of CFI, signal optimization for CFI has been an problem for traffic engineers to solve. Signal optimization models for asymmetric CFIs based on its unique geometric features were proved by simulation to be effective in providing signal progress to critical path-flows and preventing the potential queue spillover on short turning bays [42]. Monte Carlo simulation was used to find the optimal signal time to minimize delay [43]. On the basis of the explicitly built modeling of critical features and key constraints of a CFI, a model for the optimization of signal timings of a full CFI was presented [31]. In other papers, signal optimization models were presented for a two-leg asymmetric CFI design when geometric conditions were limited [42–44]. Another paper proved the design methodologies for providing pedestrian access and related pedestrian signal timings can optimize vehicular traffic performance [35]. In addition, how an Intelligent Transportation System (ITS) technology, named Transit signal priority (TSP), affects CFI design was studied [45]. A dynamic optimized method of traffic signal timing parameters was proposed considering the coordination of traffic signals between main intersections and crossovers at a CFI [34].

1.2.3. Traffic Efficiency of CFI

From the perspective of traffic efficiency, traffic simulations were used to compare the operational performance between the CFI and PFI designs, showing that the operational performance of the PFI and CFI is similar, but the CFI has a higher left-turn capacity than the PFI [26]. An accessible tool, i.e., the statistical models, was developed to assess average delay and average queue length for a CFI [46]. The results of comparisons between seven unconventional aerial intersection designs showed that the CFI design has the best operation effect on travel time [47], and another study showed that the CFI has the lowest delay among the four unconventional intersections [48]. In terms of capacity, a full CFI is better than a partial CFI [35]. In addition, signing and marking, as well as traffic safety benefits of the CFI, have also been of interest [49,50].

As mentioned above, the existing studies have consistently concluded that the traffic efficiency of CFIs is better than that of conventional intersections, and some built CFIs have achieved good results. Nevertheless, many key issues related to CFIs still need to be further studied, especially the details in the geometric design, especially the length of the displaced left-turn lane. In fact, it has a great impact on the overall operational effectiveness of CFIs, which should not be too short or too long. If it is too short, it tends to cause queue overflow when the intersection traffic is heavy; conversely, if it is too long, the signal coordination control is less effective. As can be seen from the above, on the one hand, the description in the relevant manuals is not enough sufficient, only pointing out that the length is generally within from 100 m to 150 m, and most of the relevant studies use the queue length to estimate the length of the displaced left-turn lane, so the results are not operational and difficult to be put into application; on the other hand, different traffic volumes require different lengths for the displaced left-turn lane. So far, the length of the displaced left-turn lane under various demand patterns has not been well determined, and the impact of it on the operation efficiency of the intersection is rarely considered in the current research. Therefore, it is necessary to find a common and easy-operating method to determine the length of the displaced left-turn lane for different traffic demand modes.

This paper presents a methodological procedure for evaluation and analysis of displaced left-turn lanes length based on the entropy method, with the aim of guiding the design and application of CFI. In the methodological procedure, the CFIs with different displaced left-turn lane lengths were regarded as different schemes. Aiming for sustainable transportation, six indexes obtained from VISSIM, including number of vehicles, delay, number of stops, travel time, CO emission, and fuel consumption, were used to evaluate the operational performance of these schemes. SSAM was used to evaluate the safety of CFIs schemes, and sensitivity analysis was conducted to analyze the operational performance of CFI under different traffic volumes. Finally, the methodological procedure was applied to an intersection of arterial roads in Xi'an, verifying the rationality and practicality of the methodological procedure.

The rest of the paper is organized as follows: Section 2 introduces the methodological procedure for determining the length of the displaced left-turn lane. Section 3 details the case study from Xi'an in China. Section 4 discusses and analyzes the results obtained by applying the methodological procedure of the case study. The conclusion is drawn in Section 5 to summarize the paper.

2. Methodological Procedure

2.1. Field Data Collection

To analyze the traffic flow characteristics of the intersection to be modified and to achieve the research objective, real traffic data needs to be collected. Data collection should be carried out in good weather conditions. The criteria in the intersection selection process are as follows:

(1) The selected intersection should have large amounts of left-turn traffic.
(2) There should be a limited number of pedestrians or cyclists.
(3) There is no construction area near the intersection.

The time of data collection: According to the traffic analysis report of China's major cities in the third quarter of 2020 provided by AutoNavi Traffic Big Data, the morning peak occurs between 7:00 a.m. and 9:00 a.m., the evening peak occurs between 5:00 p.m. and 7:00 p.m., and the valley (excluding late night) appears between 12:00 p.m. and 2:00 p.m. [51]. Therefore, the field data collection could be carried out during peak and valley hours on weekdays.

The data that need to be collected are as follows:

(1) The traffic volume and turning ratio, including left turns and right turns.
(2) The running speed and types of all vehicles in each lane.
(3) The current signal timing and geometric design parameters of the intersection.

2.2. Problem Analysis and Improvement Schemes Design

Analyzing the traffic characteristics of the intersection and selecting the CFI type is one of the most important parts of this study. So far, the CFI design includes four types [31]: (1) Full CFI: the main intersection is located in the center, and the four left-turn crossover intersections are located in the four approaching legs; (2) CFI-T intersection: a T-intersection that contains one CFI leg; (3) Two-leg CFI (Type A): an intersection containing displaced left-turn legs in two opposite directions, with the other two legs having the same geometry as a conventional intersection; and (4) Two-leg CFI (Type B): an intersection containing displaced left-turn legs in two perpendicular directions, the other two legs having the same geometry as a conventional intersection.

The CFI type is determined by the traffic characteristics, especially the left-turn ratio. This is because CFI is suitable for roads with large traffic volume and high left-turn ratio, setting CFI in the entrance road with low left-turn traffic volume may not bring ideal improvement effect. After determining the CFI type, to explore the length of the displaced left-turn lane for the CFI scheme, several CFI schemes with different lengths within the range suggested by the relevant manual can be regarded as different schemes and their operational performance should be compared and evaluated. One of the advantages of this method is that it is easy to apply, and the optimal scheme can be selected quickly without complicated calculations.

2.3. Development and Application of Simulation Model

2.3.1. Development of Simulation Model

Ideally, traffic data should be collected before and after the CFI application to verify the effectiveness of CFI schemes. But it is difficult to achieve in practice, especially when the CFI is not built. Therefore, simulation is an alternative option. As an effective tool to evaluate traffic engineering design and urban planning, VISSIM has become the standard of simulation software. Therefore, in this study, VISSIM is used to simulate and evaluate the schemes. Firstly, the simulation models of existing schemes and CFI schemes should be established. Secondly, to ensure the accuracy of the simulation, the geometric parameters (i.e., number of lanes, lane widths), the expected speed, traffic volumes, the traffic compositions, and the vehicle paths in the VISSIM simulation model should be consistent with the actual situation. In addition, conflict areas, reduced speed areas and signal control machines should be set up to match the actual traffic control methods and conditions in practice.

2.3.2. Calibration of Simulation Model

VISSIM parameters need to be calibrated and verified with field survey data to ensure that the simulation is consistent with the actual situation as possible [52,53]. Several calibration parameters in the VISSIM simulation model are the gap acceptance model, the car-following model, and the lane-changing model [54,55]. Capacity is mainly used to calibrate the VISSIM simulation model [56,57]. It can reflect the multiple attributes of the simulation model, and is very sensitive to the path selection behavior, so capacity is a good choice for calibration. After inputting the traffic data collected into the simulation model in VISSIM, if the capacity output from VISSIM simulation is close to the collected capacity, it can prove that the VISSIM model is accurate. The smaller the difference between the simulated capacity and the measured capacity, the more accurate the simulation model is. The mean absolute percentage error(MAPE) is generally used as an indicator to evaluate the simulation error, which can be calculated by Equation (1):

$$MAPE = \frac{1}{\mathrm{n}} \sum_{f=1}^{n} \left| \frac{C_v^f - C_a^f}{C_a^f} \right|, \tag{1}$$

where n denotes n units of vehicle flow in all directions, C_v^f denotes the simulated capacity in the VISSIM model (veh/h), and C_a^f denotes the actual investigated capacity of each flow.

2.3.3. Analysis of the Impact of CFI Applications on Traffic Operations and Environment

After calibration, the VISSIM simulation model need to be run to evaluate the operational performance and environmental impact of CFI schemes. Various evaluation indexes can be obtained from VISSIM, including operational efficiency indexes, fuel consumption, and different types of pollutant emissions. Among them, travel time, delay, and the number of stops are the most commonly used indexes [56]. With the increasingly serious traffic congestion and air pollution problems in China in recent years, sustainable development has become more and more important [58]. Therefore, the sustainable evaluation of construction projects should be carried out [59,60]. And the evaluation index for sustainable development should include not only the index of traffic conditions but also environmental protection. In this paper, six sustainable performance indicators: the travel time, delay, number of stops, number of vehicles, CO emissions, and fuel consumption are used to evaluate the operational characteristics and sustainability of CFIs.

2.4. Safety Evaluation

A complete traffic evaluation should include not only an operational assessment but also a safety assessment. The surrogate safety assessment model (SSAM), a simulation conflict analysis software developed by American scholars, is widely used in the area of traffic safety assessment [61,62]. The SSAM can analyze the simulation conflict of microscopic traffic simulation model and obtain the simulation conflict data, so as to replace the historical accident data and actual conflict data for indirect traffic safety evaluation of specific traffic facilities [53,63]. It takes the vehicle trajectory file output from the microscopic traffic simulation model as the research object, calculates various conflict analysis indicators according to certain algorithms, and uses the built-in statistical analysis function to identify, classify, and divide the severity of simulation conflicts, which can help to analyze and design safe traffic facilities. Crossing, rear end, and lane change are the three types of conflicts it outputs, which can be used to evaluate the safety of the schemes.

2.5. Sensitivity Analysis of Operational Performance

All the above steps are based on the measured traffic volume, which limits the comprehensive evaluation of different schemes in this paper. In order to cover as many traffic conditions as possible, the operation effects under different situations should be simulated. Since the objective of this paper is to select the optimal length of displaced left-turn lanes for different traffic volumes, the sensitivity analysis should mainly analyze the change of evaluation index with the change of traffic volume.

2.6. MADM Based on Entropy Method

Sustainable transportation not only requires improvement in transportation efficiency but also pollution reduction [64]. How to choose the optimal length scheme with the best operation performance and the lowest environmental pollution among several options by evaluating several separated indexes is the key problem that must be solved. Multi-attribute decision-making (MADM) is a scientific and effective method of selecting optimal alternatives considering multiple attributes, which is also known as multi-objective decision-making with limited alternatives. In the context of sustainable development, MADM is widely used in energy conservation and emission reduction assessment [65,66]. In MADM, it is generally necessary to determine the importance of indicators by calculating the weights of evaluation indicators.

The entropy method,as an objective weighting method, is widely applied to evaluate schemes with multiple factors, rather than evaluating several indicators separately [67–71]. It determines the weight of index according to the information provided by the observation value. In information theory, entropy is a measure of uncertainty. The greater the amount of information, the smaller the uncertainty and entropy. According to the characteristics of entropy, we can judge the dispersion degree of an index by entropy, and the greater the dispersion degree of an index, the greater the influence of the index on the comprehensive evaluation. Therefore, according to the variation degree of each index, the weight of each index can be calculated by information entropy, which provides the basis for the comprehensive evaluation of multiple indexes. The core of entropy method can be summarized in two parts: calculating the weights of the indicators and scoring the solutions.

2.6.1. Calculation of the Weights for the Indicators

Suppose there are a total of z groups of situations, m schemes and n indexes. The weights were calculated as follows.

Step 1: As mentioned above, each scheme has n indexes, and each index has z values. We combined the simulation results and converted them into m matrices with z*n columns M_k:

$$M_k = [V_{k,t}, D_{k,t}, S_{k,t}, T_{k,t}, C_{k,t}, F_{k,t}], \tag{2}$$

where k denotes the design scheme, $k = 1 to m$; t denotes the traffic volume combinations, $t = 1$ to z; V, D, S, T, C, and F denote the number of vehicles, delay, number of stops, travel time, CO emissions, and fuel consumption, respectively.

In the matrix M_k,

$$V_{k,t} = [V_{k,1}, V_{k,2}, V_{k,3}, \cdots, V_{k,z}]^T. \tag{3}$$

Step 2: In order to compare the simulation results of the seven schemes for each traffic volume combination, the m matrices M_1 to M_m were split and reorganized. For each traffic volume combination, the simulation results of the m schemes are combined into matrix X_t:

$$X_t = \begin{bmatrix} M_1(t,\cdot) \\ M_2(t,\cdot) \\ M_3(t,\cdot) \\ \vdots \\ M_m(t,\cdot) \end{bmatrix}, \tag{4}$$

where $M_1(t,\cdot)$ represents the t-th row of M_1, representing the value of six indexes under the t-th traffic volume combination of Scheme 1. Thus, X_t consists of m rows and n columns.

$$X_t = \begin{bmatrix} V_{1,t} & D_{1,t} & S_{1,t} & T_{1,t} & C_{1,t} & F_{1,t} \\ V_{2,t} & D_{2,t} & S_{2,t} & T_{2,t} & C_{2,t} & F_{2,t} \\ V_{3,t} & D_{3,t} & S_{3,t} & T_{3,t} & C_{3,t} & F_{3,t} \\ \vdots & \vdots & \vdots & \vdots & \vdots & \vdots \\ V_{m,t} & D_{m,t} & S_{m,t} & T_{m,t} & C_{m,t} & F_{m,t} \end{bmatrix}. \tag{5}$$

The weights of the n indexes under different traffic volume combinations are different, so z situations correspond to z sets of weights. The procedure for calculating the weights of the n indexes using the entropy method is as follows.

(1) Denote each element of the matrix X_t as y_{ij}, while X_t is denoted as Y, as shown in the following.

$$Y = \begin{bmatrix} y_{11} & y_{12} & y_{13} & \cdots & y_{1n} \\ y_{21} & y_{22} & y_{23} & \cdots & y_{2n} \\ y_{31} & y_{32} & y_{33} & \cdots & y_{3n} \\ \vdots & \vdots & \vdots & \ddots & \vdots \\ y_{m1} & y_{m2} & y_{m3} & \cdots & y_{mn} \end{bmatrix}. \tag{6}$$

Denote each column of the matrix Y by y_j:

$$y_j = \begin{bmatrix} y_{1j} & y_{2j} & y_{3j} & \cdots & y_{mj} \end{bmatrix}^T, \tag{7}$$

where m denotes the total number of schemes; n represents the total number of indexes; j denotes the j-th index.

In this way, the matrix Y can be converted into the following form:

$$Y = \begin{bmatrix} y_1 & y_2 & \cdots & y_j & \cdots & y_n \end{bmatrix}. \tag{8}$$

Among the selected six evaluation indexes, for the number of vehicles, the higher the value, the greater the capacity of the scheme, while, for the other five indexes, the lower the value, the better the scheme. In order to unify the evaluation method, the six indexes need to be processed forward or backward. We selected forward processing for the six indexes, so that a higher value represents a better result. The formula for forward processing is as follows.

$$y'_{1j} = \begin{cases} \max\{y_{1j}, y_{2j} \cdots y_{mj}\} - y_{1j}, j \neq 1 \\ y_{11}, j = 1 \end{cases}. \tag{9}$$

We denote y_j as y'_j after forward processing:

$$y'_j = \begin{bmatrix} y'_{1j} & y'_{2j} & \cdots & y'_{mj} \end{bmatrix}^T. \tag{10}$$

In this way, Y can be expressed as Y' after forward processing.

$$Y' = \begin{bmatrix} y'_1 & y'_2 & \cdots & y'_j & \cdots & y'_n \end{bmatrix}. \tag{11}$$

(2) Standardization of indicators: homogenization of heterogeneous indicators. Since the units of measurement of each index are not uniform, we should first standardize them, that is, convert the absolute value of the index to the relative value, so as to solve the

homogenization problem of different index values. The formula of standardization is as follows:

$$y''_{kj} = \frac{y'_{kj} - \min\left\{y'_{1j}, \cdots, y'_{mj}\right\}}{\max\left\{y'_{1j}, \cdots, y'_{mj}\right\} - \min\left\{y'_{1j}, \cdots, y'_{mj}\right\}} k = 1, 2, \cdots m; j = 1, 2 \cdots n. \quad (12)$$

After normalization, a new matrix Y'' is generated:

$$Y'' = \left[\begin{array}{cccccc} y''_1 & y''_2 & \cdots & y''_j & \cdots & y''_n \end{array}\right]. \quad (13)$$

(3) Calculate the proportion of scheme k in index j:

$$p_{kj} = \frac{y''_{kj}}{\sum\limits_{k=1}^{m} y_{ij}}. \quad (14)$$

Calculate the entropy of index j:

$$e_j = -\lambda \sum_{k=1}^{m} p_{kj} \ln(p_{kj}), \quad (15)$$

where $\lambda = 1/\ln(m)$, and $e_i \geq 0$.

Calculate the difference coefficient of index j.

$$d_j = 1 - e_j. \quad (16)$$

The weight of each index can be calculated by the following formula:

$$w_j = \frac{d_j}{\sum\limits_{j=1}^{n} d_j}. \quad (17)$$

The weights of all indicators under the t-th traffic volume combination are calculated and put into the matrix W_s.

$$W_s = \left[\begin{array}{cccc} w_{s,1} & w_{s,2} & \cdots & w_{s,n} \end{array}\right]. \quad (18)$$

The z sets of weights corresponding to z situations form the matrix W.

$$W = \left[\begin{array}{cccccc} W_1 & W_2 & \cdots & W_s & \cdots & W_z \end{array}\right]. \quad (19)$$

2.6.2. Evaluation and Selection of Schemes

Based on the weights of the six indexes obtained above, the scores of the seven schemes under each traffic volume combination can be calculated to find the scheme with the best performance. The specific scoring process is as follows.

(1) The weight of scheme k under indicator is calculated above. Multiply it with the weight of indicator to obtain the score of index j in scheme k.

$$q_{kj} = w_{sj} \times p_{jk}, j = 1:n; k = 1:m. \quad (20)$$

(2) The total score of scheme k can be calculated as follows:

$$q_k = \sum_{j=1}^{n} q_{kj}. \quad (21)$$

(3) The scores of all schemes under traffic combination t can be expressed as a matrix Z_s, as shown in Equation (22).

$$Q_t = \begin{bmatrix} q_1 & q_2 & \cdots & q_m \end{bmatrix}^T. \tag{22}$$

(4) The scores of all schemes under z situations form the matrix Q:

$$Q = \begin{bmatrix} Q_1 & Q_2 & \cdots & Q_t & \cdots & Q_z \end{bmatrix}^T. \tag{23}$$

In this way, the optimal scheme can be selected under each traffic volume combination.

$$A = \begin{bmatrix} k, if q_k = \max Q_1 \\ k, if q_k = \max Q_2 \\ \vdots \\ k, if q_k = \max Q_z \end{bmatrix}, k = 1 : m. \tag{24}$$

Matrix A contains z scheme numbers, representing the optimal scheme for each traffic volume combination. In this way, the optimal length of a CFI's displaced left-turn lane for different traffic volumes can be obtained.

The methodological procedure discussed above can be summarized, as in Figure 1, as follows.

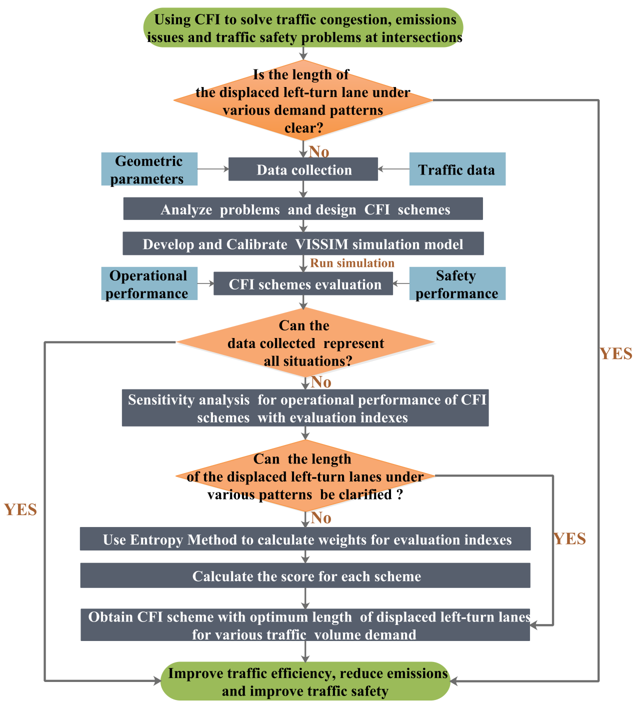

Figure 1. Methodological procedure for studying the length of the displaced left-turn lanes of Continuous Flow Intersection (CFI).

3. Case Study

3.1. Case Description

Xi'an, the capital of Shaanxi Province, has 41.7% of the high delay operation time of the road network in 2019, ranking first among the 50 major cities in China [51]. Alleviating intersection congestion in Xi'an has important implications to other cities. An intersection in the Yanta district, Xi'an, located at the junction of Dianzi 1 Road, Keji 2 Road, and Taibai South Road, is one of the typical congested intersection. It is located in the southwest of Xi'an, as shown in Figure 2, and the actual situation of the intersection is shown in Figure 3. There are many left-turning vehicles at this intersection, especially in the east–

west direction. The reason for this is, as the arterial road, Taibai South Road crosses through the Gaoxin district and serves as a daily route for commuters. A large number of vehicles from Dianzi 1 Road and Keji 2 Road merge into Taibai South Road during the peak commuting hours on weekdays. In addition, under conventional four-phase signal control, left-turning vehicles take up a portion of the green time to pass the intersection during a signal cycle, which makes the green time available for the through and left-turn vehicles of each phase very limited, so traffic congestion, traffic chaos, or even traffic paralysis always occurs in the morning and evening peak hours, which seriously affects the traffic efficiency of the intersection.

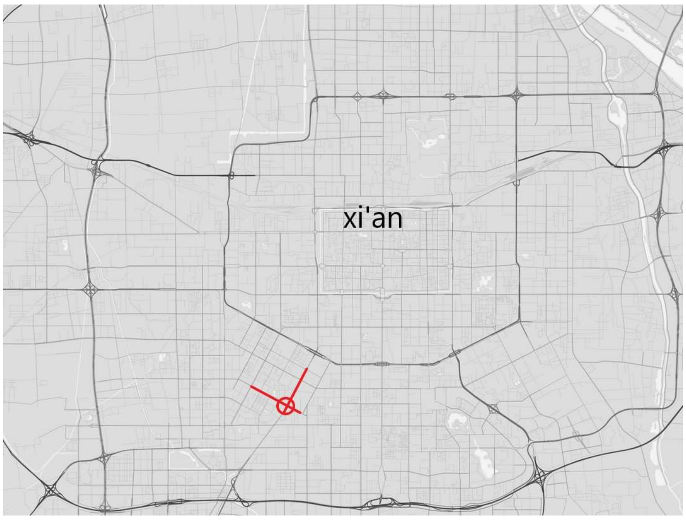

Figure 2. The location of the investigated intersection in Xi'an. The geographical background of the map can be obtained from https://alvarcarto.com/phone-background/generator/?lat=41.3942&lng=2.1708&zoom=12&mapStyle=bg-darkgray&header=Barcelona (accessed on 8 May 2021).

Figure 3. The current situation of the investigated intersection in Xi'an. Dianzi 1 Road is in the east and Keji 2 road is in the west. The north–south road is Taibai South Road. This graphic was taken by a drone at a height of 150 m. Coordinates: 108.907889474, 34.219308643.

3.2. Data Collection

The field data collection was carried out during peak and valley hours on 23 October 2020. The congestion delay index of Xi'an on 23 October 2020 is shown in Figure 4.

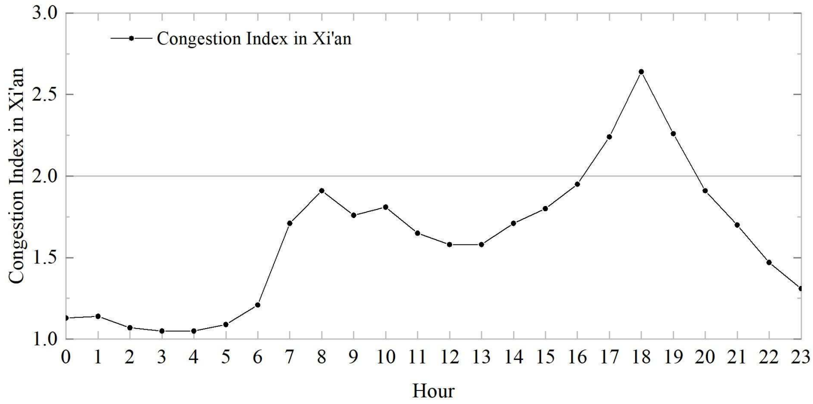

Figure 4. The congestion index in Xi'an on 23 October 2020. The real-time congestion index can be gathered from the Autonavi Company at https://report.amap.com/detail.do?city=610100 (accessed on 8 May 2021).

A drone, a smartphone, and two radars were used to collect data, with the former two used for the vehicle count and the latter for collecting the operating speeds of vehicles. The collected traffic volume is listed in Table 1.

Table 1. Collected data during investigation.

Item	Morning Peak Hour	Noon Valley Hour	Evening Peak Hour
Traffic volume (veh/h)	7935	7857	6335

Traffic volume in the morning peak hour is highest, so it is selected as the representative traffic volume, the detailed data of which is listed in Table 2.

Table 2. Collected data during the morning peak hour.

Item	Flow	Flow Number	Car	Bus	Truck	Average Speed (km/h)	Max.Speed (km/h)	Min.Speed (km/h)
Westbound	Left-turn	1	390	7	0	31.68	70.56	0
	Through	2	570	36	0			
	Right-turn	3	79	22	0			
Eastbound	Left-turn	4	346	0	0	22.32	63.72	0
	Through	5	714	36	0			
	Right-turn	6	115	0	0			
Southbound	Left-turn	7	137	7	7	15.48	54	0
	Through	8	2085	79	22			
	Right-turn	9	455	29	0			
Northbound	Left-turn	10	87	0	0	9.0	29.88	0
	Through	11	2330	43	7			
	Right-turn	12	332	0	0			

In this table, 0 km/h means the stops of vehicle, which would occur in the following two situations: (1) The traffic lights in the direction for the vehicle are red, so the vehicle needs to stop and wait; (2) The congestion is too severe to move for vehicles, so even the traffic lights in the direction for the vehicle are green.

The collected data show the following characteristics:

(1) The left-turn ratio of vehicles traveling westbound and eastbound is higher than that of vehicles traveling southbound and northbound.

(2) The vehicles' running speed varies greatly, and the average running speed of vehicles in four directions is far below the speed limit (60 km/h).

(3) Cars account for most of the vehicles.

3.3. Design Scheme Description and Geometry Layout

3.3.1. Design Scheme Description

The collected data shows there are fewer left-turning vehicles in the northbound and southbound directions, so the geometric layout of CFI for this intersection in these two directions is kept unchanged, and only the geometric layout in the eastbound and westbound directions is redesigned. This kind of CFI is called a two-leg CFI (Figure 5b).

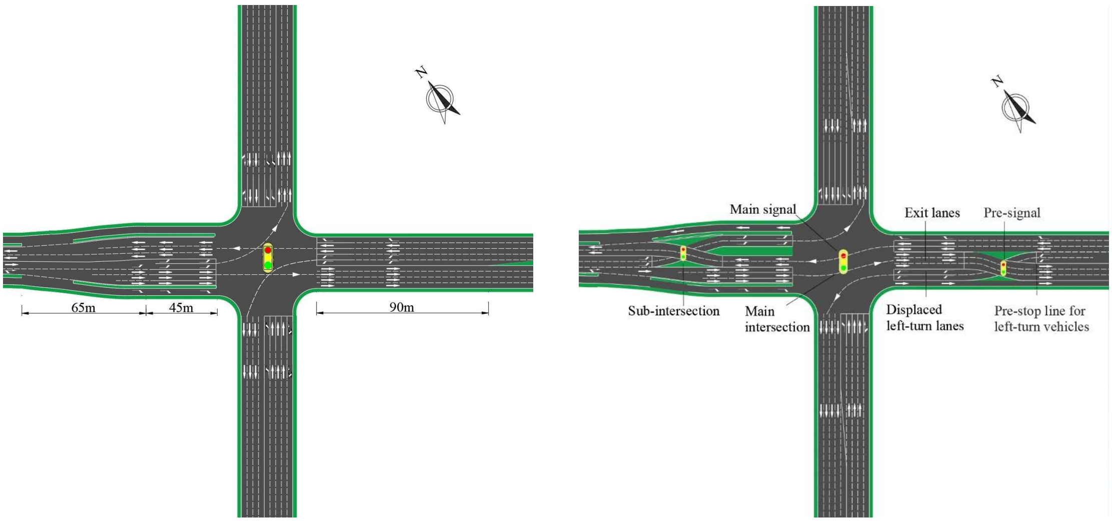

(**a**) Illustration of the existing design. (**b**) Illustration of the two-leg CFI scheme.

Figure 5. Illustration of the existing design and the two-leg CFI scheme.

Figure 5a is an illustration of the current situation of the intersection, with two left-turn lanes at the west and east approach, and the width of each lane in all approaches is 3 m. A widening transition section with a length of 65 m exists in the west entrance. Figure 5b shows the redesigned two-leg CFI scheme based on the existing road conditions and space resources, and it redistributes the right to use existing lanes without adding additional left-turn lanes. In order to control the variables, in the two-leg CFI scheme, the number of lanes in each direction is consistent with the existing scheme. It is not possible that the length of a displaced left-turn lane is always in the range of 100∼150 m [38], so we extended the range to 50∼200 m and considered six lengths, creating six different schemes, to determine which length of the displaced left-turn lane for the two-leg CFI scheme is most applicable to the above intersection. The length ranges from 50 to 200 m, with intervals of 30 m. The six schemes are denoted as Scheme 2 to Scheme 7. Scheme 1 is the existing design as a benchmark for comparison.

Figure 6 shows the paths of vehicles in the two-leg CFI, taking the westbound direction as an example. The flows $f = 2$ and $f = 5$ are the through traffic in the East to West (EW) and West to East (WE) lanes, respectively, which are the main traffic flow with relatively heavy traffic, and the flows $f = 1$ and $f = 4$ are left-turn traffic in the East to South (ES) and North to East (NE) lanes, respectively. The main difference between CFI and conventional intersection lies in the path of left-turn and through vehicles. For through vehicles, they need to pass through two intersections: the main intersection and the pre-intersection. After arriving at the main intersection, if the main signal light for through is green, the through vehicles directly pass through the main intersection and arrive at the pre-intersection. At this time, the pre-signal for through is also green after the signal coordination control, so the through vehicles can pass through the main intersection and pre-intersection continuously.

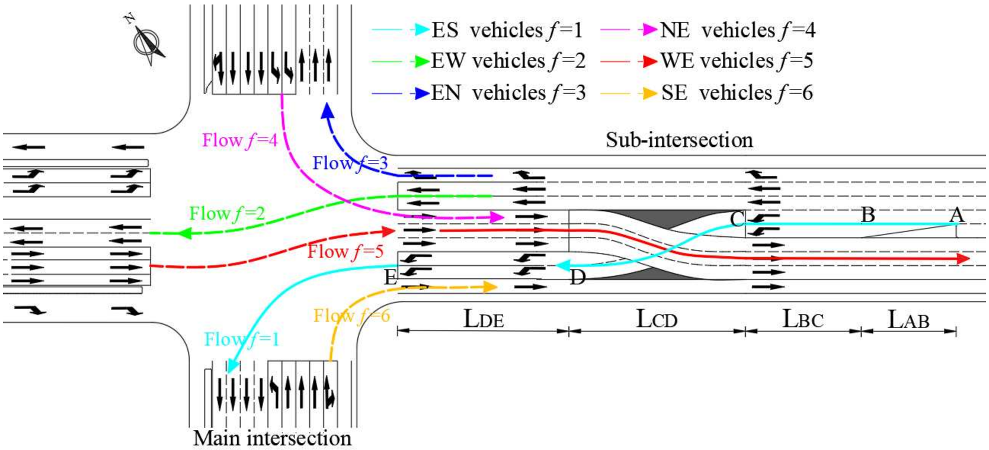

Figure 6. The paths of vehicles in the two-leg CFI. In the figure, W, E, N, and S are abbreviations of West, East, North, and South, respectively, and the arrows with different colors show six different flows. For example, ES denotes east to west traffic flow.

It is more complex for left-turn traffic flow to complete left-turn at CFI, and the whole process can be divided into two steps. Step 1: The vehicles in flow $f = 1$ drive to the left-turn stop line before the pre-intersection; if the pre-signal for left-turn is green, they will pass through the pre-intersection and enter the displaced left-turn lanes and arrive at the main intersection. If the signal light at pre-intersection is red, wait. Step 2: When the left-turn vehicles arrive at the main intersection, if the through light is turning on, they will leave the main intersection. The right turning flows $f = 3$ and $f = 6$ operate in the same way as conventional intersections. Compared with the existing scheme, the two-leg CFI schemes eliminate the special phases for left turning in the eastbound and westbound directions, turning the four-phase control of the main intersection into a three-phase control.

3.3.2. Geometry Layout

The geometrical parameters of the two-leg CFI are shown in Figure 6 and Table 3, taking the design of the eastbound lanes as an example. Section AB widens a left-turn lane by compressing the green belt, and Section BC stores the left-turn vehicles arriving in a pre-signal period. The vehicles cross the CD section and reach the displaced left-turn lane during the through vehicles crossing the intersection in the south and north directions. The ED segment is used to store the vehicles passing when the signal light for a left turn at the pre-intersection is green.

Table 3. Geometric parameters of the two-leg CFI.

Item	Description
L_{AB}	30 m. Length for widening a left-turn lane.
L_{BC}	100 m. The queue length of left-turn vehicles during the period when the pre-signal light for left turns is red.
L_{CD}	45 m. Length of left-turn vehicles crossing from the BC segment to the displaced left-turn lane DE.
L_{DE}	50 m/80 m/110 m/140 m/170 m/200 m in Scheme 2 to Scheme 7, respectively. Wait area length in case of flow needing to wait to turn left.

The lengths of all the sections described above are based the 'Policy on Geometric Design of Highways and Streets' [72]. The lengths of all sections were input into the VISSIM simulation model to evaluate the performance of the CFI design at a design speed of 60 km/h.

3.4. VISSIM Calibration and Calculation of Operational Measures

3.4.1. Calibration Results

Based on the VISSIM calibration method proposed above, we calibrated the established model with the collected data. The calibration results and calculated MAPEs are shown in Table 4.

Table 4. VISSIM simulation calibration results.

Direction	Westbound			Eastbound			Northbound			Southbound		
Flow	LT	TH	RT	LT	TH	RT	LT	TH	RT	LT	TH	RT
Investigated capacity (veh/h)	397	606	101	346	750	115	87	2381	332	152	2186	483
Simulated capacity (veh/h)	400	632	107	370	749	117	78	2004	331	146	2063	486
Individual MAPE (%)	0.76	4.29	5.94	6.94	−0.13	1.74	−10.34	−15.83	−0.30	−3.95	−5.63	0.62
MAPE (%)							4.71					

In this table, 'LT', 'TH', and 'RL' denote 'Left-Turn', 'Through', and 'Right-Turn' vehicles, respectively.

The error between the capacity in the VISSIM simulation model and the actual capacity is 4.71%, which shows that the calibrated VISSIM simulation model provides a reasonable capacity estimation. The estimated error is considered acceptable in a practical engineering application [57,73].

3.4.2. Simulation Results

A total of 7 simulations were carried out: the existing scheme and the six two-leg CFI schemes. The collected data listed in Table 3 were input into the VISSIM simulation model. The simulation results were used to evaluate the operation effect of six two-leg CFI designs, as shown in Table 5.

Table 5. Operational performance of seven schemes with morning peak hour data.

Scheme	Item	Number of Vehicles (Veh/h)	Delay (s)	Number of Stops (Times/Veh)	Travel Time (s)	CO Emissions (Grams/h)	Fuel Consumption (Gallons/h)
1	Result	7472	55.515	0.783	108.079	19061.405	272.695
2	Result	8017	34.078	0.678	76.078	17756.766	254.031
	Rate	7.29%	−38.61%	−13.51%	−29.61%	−6.84%	−6.84%
3	Result	8037	34.306	0.685	76.657	17853.019	255.408
	Rate	7.56%	−38.20%	−12.54%	−29.07%	−6.34%	−6.34%
4	Result	8037	34.157	0.688	76.148	17853.545	255.415
	Rate	7.56%	−38.47%	−12.22%	−29.54%	−6.34%	−6.34%
5	Result	8037	33.879	0.684	75.935	17811.231	254.81
	Rate	7.56%	−38.97%	−12.64%	−29.74%	−6.56%	−6.56%
6	Result	8076	33.809	0.684	77.701	18288.07	261.632
	Rate	8.08%	−39.10%	−12.71%	−28.11%	−4.06%	−4.06%
7	Result	8037	33.655	0.684	75.749	17786.818	254.461
	Rate	7.56%	−39.38%	−12.64%	−29.91%	−6.69%	−6.69%

In this table, rate indicates (two-leg CFI scheme-existing scheme)/existing scheme×100%, and a positive value indicates an increase in the value of the evaluation index, while a negative value indicates a decrease in the value of the evaluation index.

According to the simulation results, the number of vehicles of the six schemes simulated with the measured traffic data is greater than that of the existing scheme, which indicates that two-leg CFIs with different lengths of displaced left-turn lane can improve the capacity of the intersection, but the improvement degree between the six schemes has no significant change. Among the six indexes, the improvement in delay is the most significant, followed by travel time. The delay and travel time of the six schemes were reduced by at least 38% and 29%, respectively, and the improvement rate of Scheme 6 is the highest. This shows that the two-leg CFIs have a good performance in improving traffic efficiency. All six schemes can reduce the number of stops at intersections, but they have similar degrees of improvement, with a maximum improvement rate of 13.51% obtained in Scheme 2. In each scheme, CO emissions and fuel consumption showed the same improvement ratio. Compared with Scheme 1, all six schemes can reduce CO emissions and fuel consumption with a maximum improvement ratio of 6.84%. Although the improvement rate is not high, it still shows that the CFI has an optimization effect on the environment. The above analysis shows that CFI schemes with different displaced left-turn lane lengths not only have considerable potential to improve intersection efficiency but also to reduce environmental pollution caused by vehicle emissions to a certain extent.

3.5. Safety Evaluation

Based on the safety evaluation method described above, we imported the ".trj" file output from VISSIM into SSAM software and obtained the conflict simulation results of the the existing scheme and six two-leg CFI schemes. The results are shown in Table 6.

Table 6. Safety analysis of seven simulations by the surrogate safety assessment model (SSAM).

Scheme Number	Item	Crossing	Rear End	Lane Change	Total
1	existing scheme	19	35	33	86
2	two-leg CFI 50 m	9	56	24	89
3	two-leg CFI 80 m	2	49	24	75
4	two-leg CFI 110 m	2	49	24	75
5	two-leg CFI 140 m	2	46	22	70
6	two-leg CFI 170 m	2	45	23	71
7	two-leg CFI 200 m	2	45	25	73

The results show that the two-leg CFI design schemes significantly reduce "crossing" and "lane change" compared to the existing conventional scheme, especially "crossing". Specifically, crossings occur 19 times in the existing scheme, but they generally occur only twice in the two-leg CFI schemes, which can be attributed to the pre-intersections and pre-signals alleviate the conflicts between left-turning vehicles and through vehicles at the main intersections. The "lane change' in the two-leg CFI schemes is reduced by 28% compared with the existing scheme. In terms of rear end, on average, the conflict frequency of the "rear end" two-leg CFI scheme is 38% greater than that of the existing scheme, indicating that a two-leg CFI may increase the likelihood of "rear end". In general, the total number of conflicts of the two-leg CFI scheme is less than that of the existing scheme, indicating that the two-leg CFI shows a greater advantage in safety assessment.

Combining the above operational effectiveness and safety analysis results, the six two-leg CFI schemes exhibit different optimization effects. Overall, the longer the length of the shifted left-turn lanes, the higher the optimization effect, but this conclusion is obtained using the collected traffic data and it cannot represent all cases, which limits the evaluation of the operation effects of the different two-leg CFI schemes. In order to cover as many traffic conditions as possible, the operation effects under different situations should be simulated and compared with the existing scheme to make a comprehensive evaluation of the two-leg CFI schemes.

3.6. Sensitivity Analysis of Operational Performance

Sensitivity analysis mainly analyzes the change in the six indicators for evaluation, such as the number of vehicles, delay, travel time, number of stops, CO emissions, and fuel consumption, along with the traffic volume. In the sensitivity analysis, the traffic parameters collected in the morning peak were used in all simulations. Only the traffic volume was changing, which was determined by Volume-to-Capacity ratio(V/C), the ratio of flow rate to capacity for a system element. The basic numbers of lanes in the westbound, eastbound, northbound, and southbound directions of the intersection are four, two, four, and five, respectively. When the design speed is 60 km/h, according to the "Highway Capacity Manual" [74], the maximum capacity for two lanes, four lanes, and five lanes, corresponding to the service level E in the city, is 1780 veh/h, 3560 veh/h, and 4450 veh/h, respectively. The V/C for traffic volume ranges from 0.2 to 1.0 in the westbound and eastbound directions and changes within a V/C from 0.5 to 0.9 in the northbound and southbound directions simultaneously with an increase of 0.1 V/C in all directions. All the traffic parameters in VISSIM are shown in Table 7. The signal timing for the existing scheme and two-leg CFI schemes under 45 volume combinations were calculated by synchro7.

Table 7. Parameters input into sensitivity analysis in VISSIM.

Item	Value
Car/Bus/Truck ratio	1039:65:0(WB)/1176:35:0(EB)/2750:43:7(NB)/2677:115:29(SB)
Left-turn/Through/Right-turn ratio	397:606:101(WB)/346:750:115(EB)/87:2381:332(NB)/152:2186:483(SB)
Eastbound volume (veh/h)	356/534/712/890/1068/1246/1424/1602/1780
Westbound volume (veh/h)	712/1068/1424/1780/2136/2492/2848/3204/3560
Southbound volume (veh/h)	2225/2670/3115/3560/4005
Northbound volume (veh/h)	1780/2136/2492/2848/3204

The southbound(SB) and northbound(NB) traffic volume changes simultaneously, and the eastbound(EB) and westbound(WB) traffic volume changes simultaneously, too. In this paper, t denotes t-th traffic volume combination, which takes values from 1 to 45. For example, $t = 1$ denotes 356 veh/h (EB volume) $\times$ 712 veh/h (WB volume) $\times$ 2225 veh/h (SB volume) $\times$ 1780 veh/h (NB volume).

Sensitivity analysis can reflect the improvement ratio of two-leg CFI schemes compared to the present scheme. The six indexes mentioned above are still selected as indexes for evaluation. Take Scheme 2 as an example, where the improvement ratio is calculated by ratio = (Scheme 2 $-$ Scheme 1)/Scheme 1 $*$ 100% or ratio = (Scheme 1 $-$ Scheme 2)/Scheme 1 $*$ 100%. The former is used to calculate the improvement ratio of the number of vehicles, and the latter is used to calculate the other indicators. A positive value in the sensitivity analysis indicates that the CFI schemes improves the traffic operation, while a negative value indicates the opposite.

Figure 7 shows the improvement ratio of the number of vehicles in six two-leg CFI schemes compared with Scheme 1 (present scheme). Overall, the improvement ratio for the number of vehicles in the six schemes shows the same trend: It increases with the increase of the traffic volume, and, when the traffic volume is low (V/C in eastbound and westbound is less than 0.5), the improvement for the number of vehicles is negative optimization and irregular. In addition, the improvement degree of the number of vehicles is between -3% and 18%, and it can be found that, when the traffic volume is the heaviest, the maximum improvement proportion appears in Scheme 5 and Scheme 7, with the value of 18%.

Figure 8 shows the improvement ratio of the delay of six two-leg CFI schemes compared with Scheme 1 (present scheme). In general, under any combination of traffic volume, the improvement rate for delay in all two-leg schemes is more than 10%, and greater than 25% in most cases, indicating that the CFI schemes have a significant advantage in reducing delay compared to existing schemes. As with the number of vehicles, the improvement ratio of delay increases with the increase of traffic volume in any scheme, with a maximum reduction in delay of 45% in the best case.

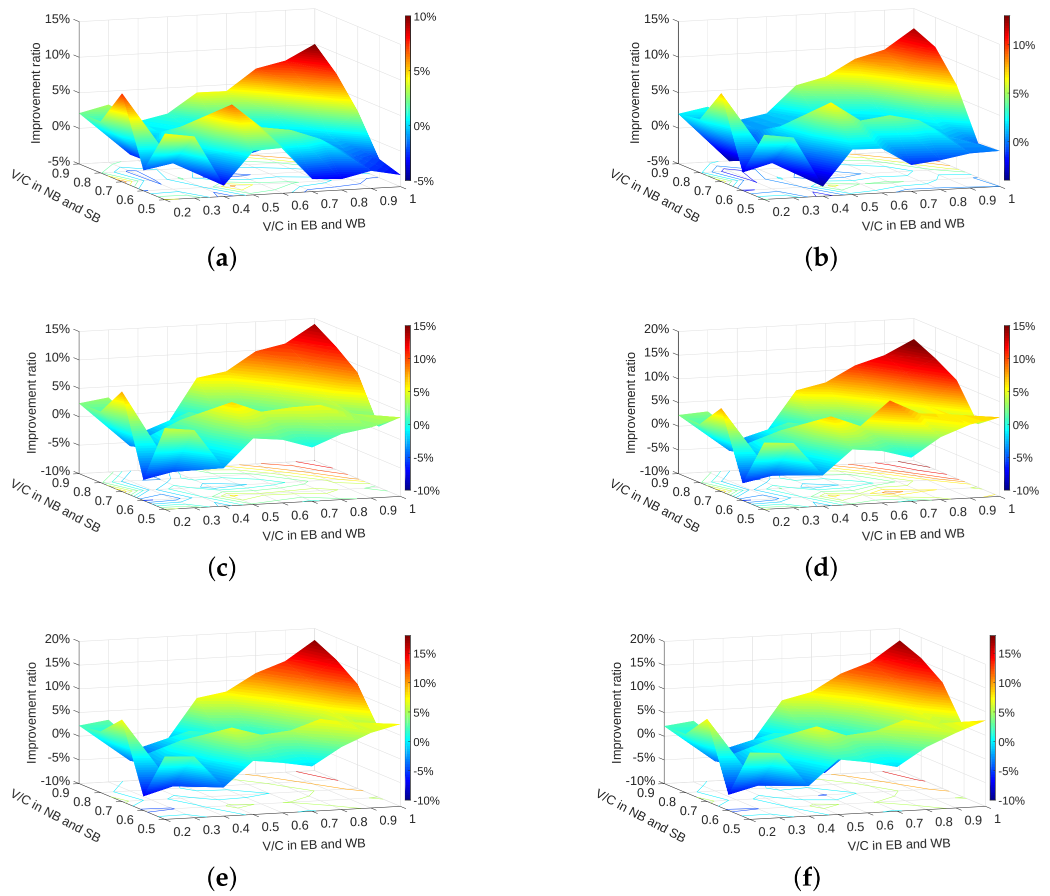

Figure 7. Improvement ratio of the number of vehicles. (**a**) Scheme 2, (**b**) Scheme 3, (**c**) Scheme 4, (**d**) Scheme 5, (**e**) Scheme 6, (**f**) Scheme 7. In the figure, EB, WB, NB, SB and V/C denote Eastbound, Westbound, Northbound, Southbound and Volume-to-Capacity ratio, respectively.

Figure 9 shows the improvement ratio for the number of stops of six two-leg CFI schemes compared with Scheme 1 (present scheme) and the improvement ratio of all schemes has several common characteristics: (1) The improvement ratio fluctuates between −28% and 25%, indicating that, in some cases, the number of stops in two-leg CFI schemes is more than that in existing schemes. (2) On the whole, in all schemes, the improvement ratio increases with the increase of traffic volume in the northbound and southbound direction. (3) When V/C in eastbound, westbound, southbound, and northbound are greater than 0.7, the improvement ratio drops sharply from positive value to negative value.

Figure 10 shows the improvement ratio for the travel time of six two-leg CFI schemes compared with Scheme 1 (present scheme). As with the delay, the improvement for travel time in each scheme is positively optimized under any combination of traffic volume, ranging from 14% to 35%, and the heavier the traffic volume is, the higher the improvement ratio of travel time is. In addition, from the range of improvement degree of each scheme, the minimum and maximum values of travel time improvement ratio improve as the length of the displaced-left turn lanes increases.

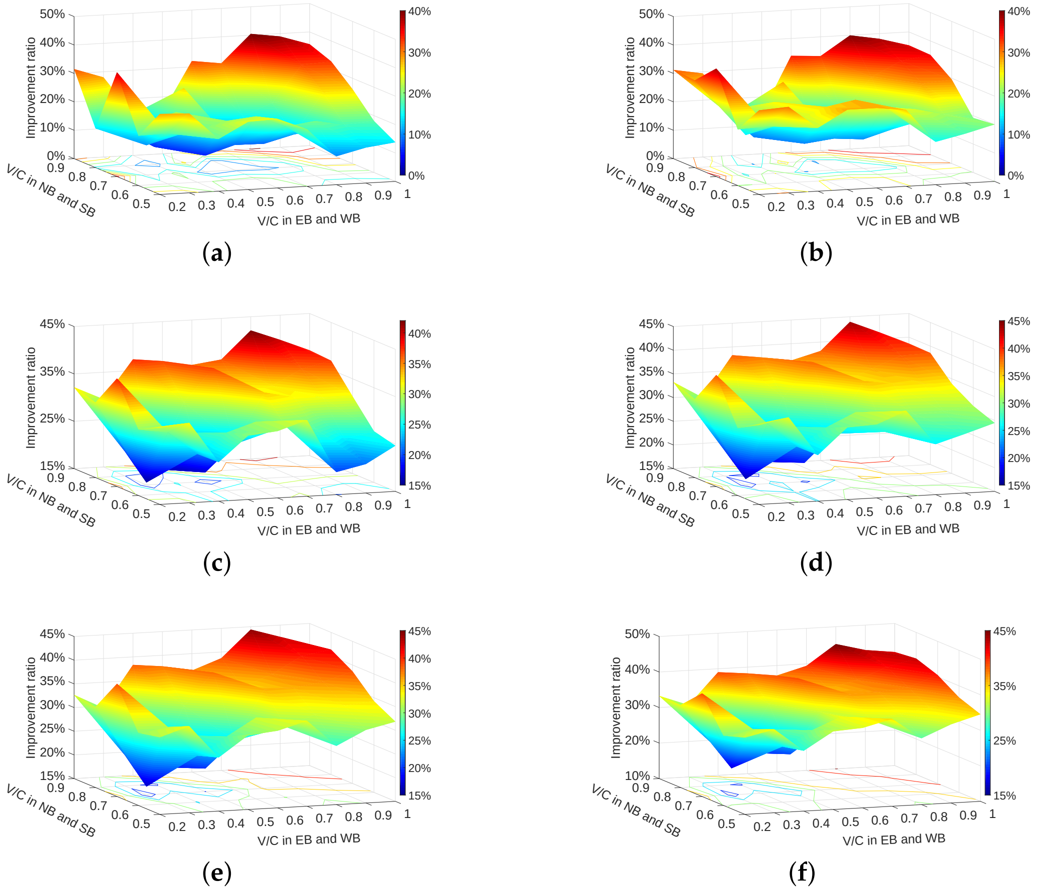

Figure 8. Improvement ratio of the delay. (**a**) Scheme 2, (**b**) Scheme 3, (**c**) Scheme 4, (**d**) Scheme 5, (**e**) Scheme 6, (**f**) Scheme 7. In the figure, EB, WB, NB, SB and V/C denote Eastbound, Westbound, Northbound, Southbound and Volume-to-Capacity ratio, respectively.

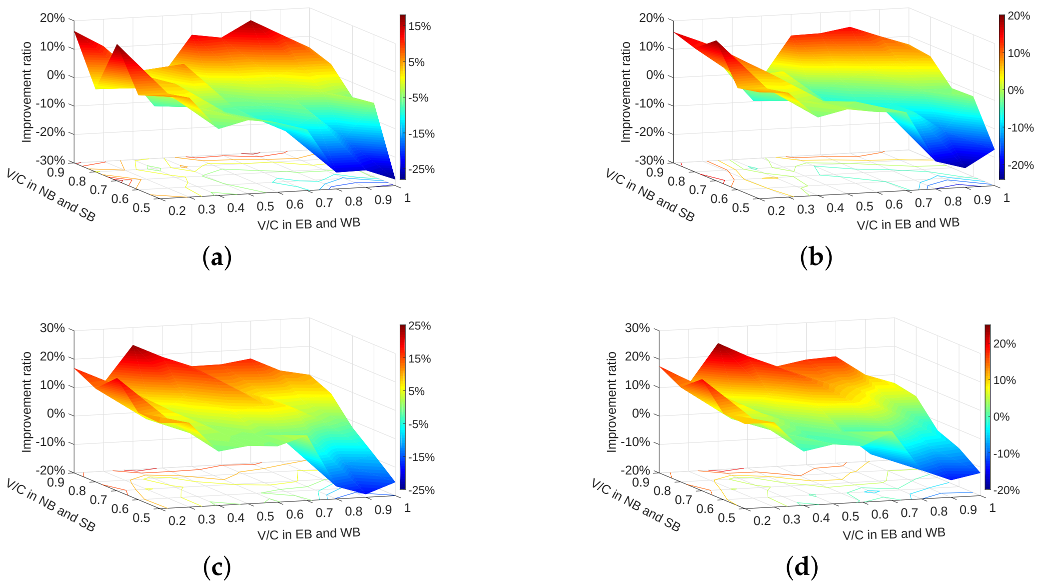

Figure 9. *Cont.*

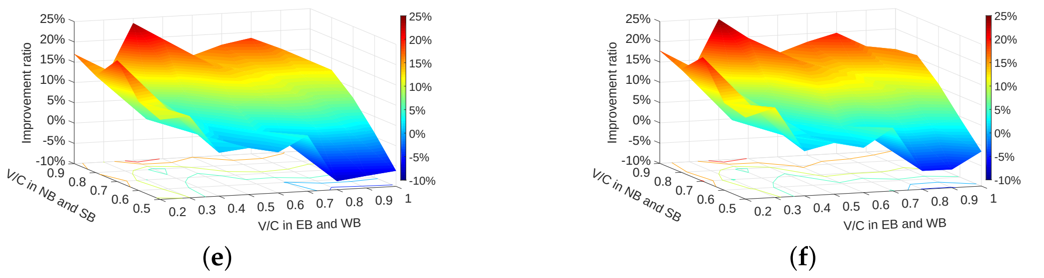

Figure 9. Improvement ratio of the number of stops. (**a**) Scheme 2, (**b**) Scheme 3, (**c**) Scheme 4, (**d**) Scheme 5, (**e**) Scheme 6, (**f**) Scheme 7. In the figure, EB, WB, NB, SB and V/C denote Eastbound, Westbound, Northbound, Southbound and Volume-to-Capacity ratio, respectively.

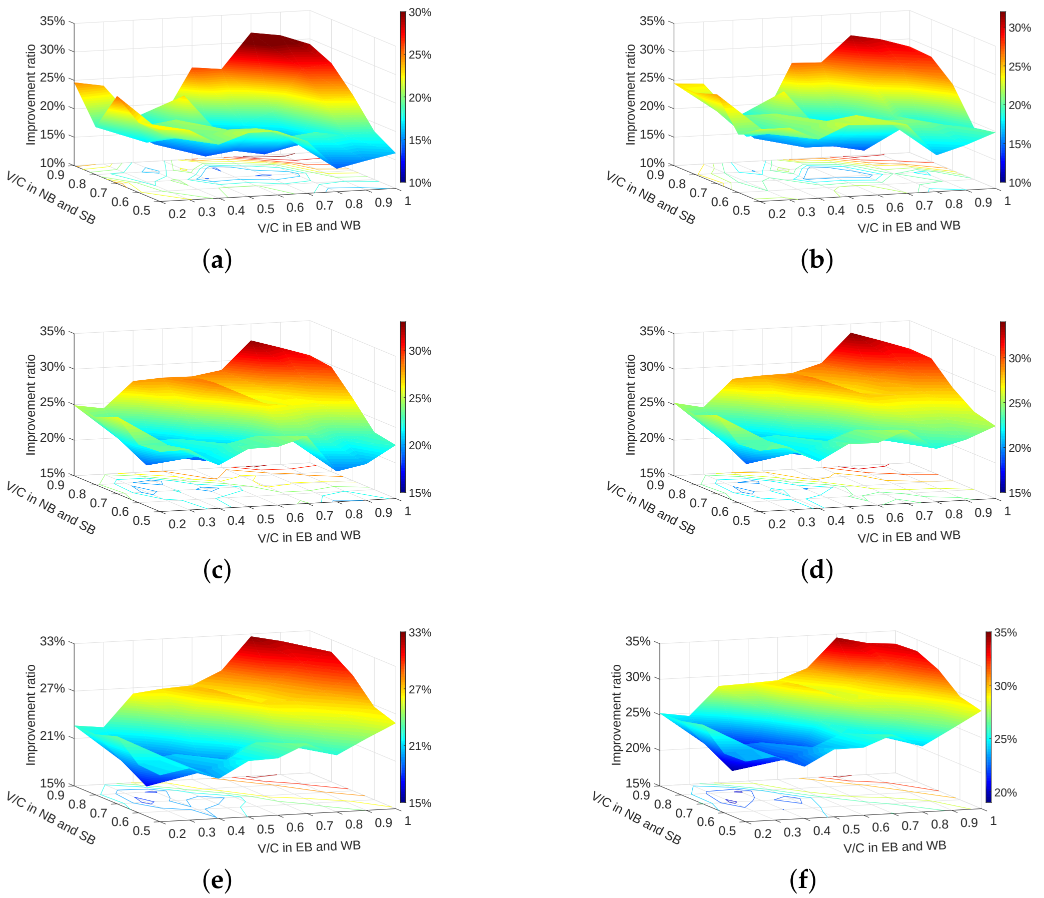

Figure 10. Improvement ratio of the travel time. (**a**) Scheme 2, (**b**) Scheme 3, (**c**) Scheme 4, (**d**) Scheme 5, (**e**) Scheme 6, (**f**) Scheme 7. In the figure, EB, WB, NB, SB and V/C denote Eastbound, Westbound, Northbound, Southbound and Volume-to-Capacity ratio, respectively.

Figure 11 shows the improvement ratio for the CO emissions and fuel consumption of six two-leg CFI schemes compared with Scheme 1 (present scheme). The trend of improvement ratio for CO emissions and fuel consumption in different schemes shows the same characteristics: (1) The improvement ratio increases with the increase of V/C in the northbound and southbound directions. (2) In most cases, the improvement degree of CO emissions and fuel consumption is positive; only in a small number of cases is the improvement ratio of CO emissions and fuel consumption less than 0, with the maximum negative optimization of 5% under the worst case, indicating that two-leg CFI schemes can reduce emissions and fuel consumption while increasing the number of vehicles, further reflecting the superiority of CFI scheme in improving traffic efficiency.

In summary, the results of sensitivity analysis showed the following characteristics:

(1) The two-leg CFI designs can improve the six indexes to varying degrees, with the highest percentage of improvement in delay, up to 45%, followed by travel time. The number of vehicles, the number of stops, the CO emissions, and fuel consumption of the two-leg CFI schemes are better than those of the existing scheme for most traffic volume combinations, indicating the two-leg CFI schemes not only have high traffic benefits but also considerable potential in environmental benefits.

(2) In general, the degree of improvement of the six indicators increases with the increase in traffic volume, meaning the two-leg CFI has higher benefits under a high traffic demand.

(3) All the six indicators are independent, and they may achieve the maximum improvement ratio in different scenarios under the same traffic volume combination, respectively, so it is difficult to obtain the optimal solution for each traffic volume combination directly from the sensitivity analysis. Therefore, it is necessary to use MADM to make decisions.

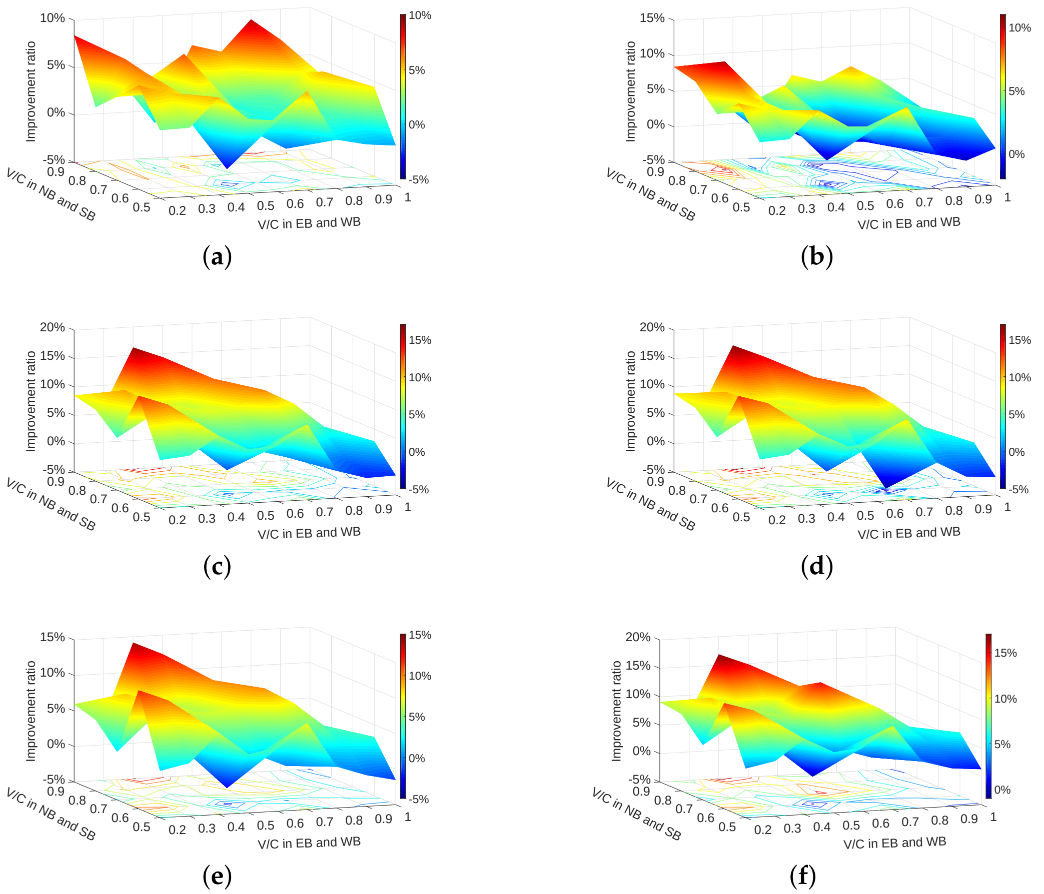

Figure 11. Improvement ratio of the CO Emissions and Fuel Consumption. (**a**) Scheme 2, (**b**) Scheme 3, (**c**) Scheme 4, (**d**) Scheme 5, (**e**) Scheme 6, (**f**) Scheme 7. In the figure, EB, WB, NB, SB and V/C denote Eastbound, Westbound, Northbound, Southbound and Volume-to-Capacity ratio, respectively.

4. Results and Discussion

According to the sensitivity analysis and MADM based on the entropy method, we obtained the two-leg scheme corresponding to the optimal length of displaced left-turn lanes under different traffic volume combinations. In order to present the results in a way corresponding to the way the traffic volume combinations change, we convert matrix A into a 9×5 matrix, with each color representing one scheme, and the number 1 represents the existing scheme, and 2, 3, 4, 5, 6, and 7 represent the six two-leg CFI schemes, respectively. The results are displayed in Figure 12.

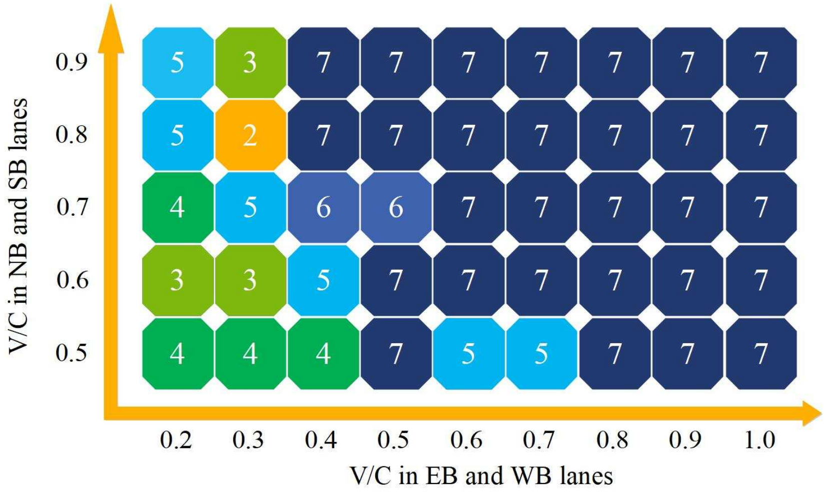

Figure 12. The optimal scheme for 45 traffic volume combinations. The numbers in the figure represent the scheme with the best performance among the six schemes for one volume combination.

It can be found that Scheme 1, the existing scheme, does not appear under any situation in Figure 12, meaning all six two-leg CFI schemes perform better than the existing scheme.

Scheme 2 occupies only one block, indicating the two-leg CFI scheme with a 50 m displaced left-turn lanes performs poorly overall.

Scheme 3 and Scheme 4 are mainly distributed in the lower left of Figure 12, occupying only seven blocks in total. And they are concentrated in the area where the V/C in westbound and eastbound lanes is less than 0.4. This indicates Scheme 3 and Scheme 4 are suitable for low traffic volume.

In the whole scale, Scheme 5, the one mainly distributed in the lower left corner of the figure, occupies 6 blocks, and it is the recommended scheme for these 6 traffic volume combinations.

Scheme 6 is distributed in the left and center of the figure, but it occupies only 2 blocks and occurs when the V/C in northbound and southbound lanes is 0.7.

Scheme 7, which is the one with a displaced left-turn lane of 200 m, occupies most of the area of the figure where the V/C in westbound and eastbound lanes exceeds 0.5, implying that Scheme 7 seems to be the optimal solution in these cases, but it cannot be denied that the two-leg CFI with a longer displaced left-turn lanes length would perform better under these conditions for the studied intersection, indicating that the results of the scheme selection matrix are no longer of high guiding significance in the choice of the displaced left-turn lane length when the V/C in westbound and eastbound lanes is greater than 0.5. However, it is uneconomical and unrealistic to increase the length of the displaced left-turn lanes blindly. Through the investigation, most of the urban road intersection spacing ranges from 400 m to 500 m, or even shorter. The displaced left-turn lanes of 200 m is close to half of the urban road intersection spacing, which is obviously unreasonable. In this case, other methods should be sought to improve the efficiency of the intersection, such as widening the road, increasing the left-turn lanes, and other solutions.

In general, the heavier the traffic volume is, the longer the length of the displaced left-turn lanes is required. For the studied intersection, when the V/C in westbound and eastbound lanes is less than 0.5, a displaced left-turn lanes length of 80$\sim$170 m is applicable, and it can be selected in the scheme selection matrix according to the road resources and traffic volume; meanwhile, when the V/C in westbound and eastbound lanes exceeds 0.5, the improvement effect of traffic efficiency can no longer rely on increasing the displaced left-turn lanes, which may be the result of an overly high proportion of left-turn vehicles in the eastbound and westbound lanes of this intersection.

According to the above results, the entropy method-based MADM can provide a sustainability assessment method for the achievement of sustainability objectives for CFI schemes with different displaced left-turn lanes lengths, and its results are reliable, because six sustainable performance indicators from three aspects were chosen to evaluate the sustainability of CFI schemes and the optimal CFI schemes with the selected displaced left-turn lanes could balance the traffic efficiency and environmental pollution to the maximum extent. In addition, this methodological procedure achieves the goal of improving the sustainability of transportation infrastructure in the design and planning stage, especially for roads and unconventional intersections, and through the schemes evaluation, the green design that can maximize traffic efficiency and reduce carbon emissions while making rational use of land resources can be obtained.

As a sustainability improvement method to alleviate traffic congestion and environmental pollution at urban intersections, CFIs can make full use of existing lane configuration, improve the traffic efficiency of intersections and reduce exhaust emissions, and its application is of great significance to promote the development of green roadways and sustainable transportation infrastructure.

5. Conclusions

Sustainable transportation is one of the current goals of urban development. And it should be emphasized that the concept of sustainability is not a supplementary element to sustainable transportation, but it is necessary to achieve function, economic, and traffic efficiency at intersections in order to achieve energy conservation and emission reduction while meeting the current and future traffic demand. China is still in the rapid development stage of urbanization; with rapid increases in private vehicles and urban population, the traffic conditions at intersections need to be improved urgently to increase the sustainability of the road. Following relevant manuals, applying the concept of sustainable development with local characteristics and constructing green road designs consistent with land resources is one of the most important ways to achieve the goal of road sustainability.

A CFI, as one of the sustainable unconventional intersections to solve the urban traffic problems, has great advantages in reducing the signal phase number and delay and in improving traffic capacity. Since the length of the displaced left-turn lanes under various demand patterns has not been well determined, this paper presents a methodological procedure for determination and evaluation of displaced left-turn lanes' length. In the methodological procedure, the operational and safety performance of the CFI schemes were simulated and evaluated by VISSIM and SSAM. The weights determination of sustainable performance indicators and the selection of CFI schemes with different displaced left turn lanes' lengths are performed through the entropy method and MADM. The approach to select the optimal displaced left-turn lane length for the CFI is possible because it combines attributes, such as traffic efficiency, environmental metrics, and fuel consumption. Moreover, the MADM and the entropy method used in this study are easy to understand and can be applied by engineers to determine which two-leg CFI scheme should be adopted if given different conditions.

The results of the case study show that the two-leg CFI scheme has an improvement effect on all six sustainable performance indicators, with the greatest improvement in delay and travel time. In the best case, compared with the conventional intersection, the number of vehicles increases by 13%, and the delay, travel time, number of stops, CO emission, and fuel consumption decrease by 41%, 29%, 25%, 17%, and 17%, respectively. The results of sensitivity analysis show that the greater the traffic volume is, the longer the displaced left-turn lanes should be. However, in some cases, the design of CFI with a long displaced left-turn lane is not necessarily the best way to improve the traffic efficiency of the intersection, and other solutions need to be found to improve the sustainability of urban roads. In addition, the case study proves that the methodological procedure is valid and feasible, and the results of the length of the displaced left-turn lanes in this paper only pertain to the studied intersection, the same procedure can be used to other intersections, as well as other traffic problems.

Sustainable transportation and sustainable transportation infrastructure will always be the theme of transportation development in the future, both from the perspective of society and economy, as well as from the perspective of environment and climate, because sustainable development needs a transportation system that can not only reduce traffic congestion and accidents but also reduce pollution and energy consumption. If CFI and other sustainable transportation infrastructure can be extended to the whole city or even the entire country, it will have a profound impact on the society, economy, and environment.

Limitations of the research: (1) Throughout the analysis of this research, only changes in traffic volumes were considered. In fact, the left turning ratio and vehicle type ratio have a significant effect on the operational effectiveness of CFI. However, it was not considered in this research. A sensitivity analysis of the left-turn ratio and vehicle type ratio can be done in future research to investigate the effects of these two factors on the length of the displaced left-turn lane of CFI. (2) It is mentioned in this research that, in some cases, the design of CFI with long displaced left-turn lane length is not necessarily the best way to improve the traffic efficiency of intersections. However, due to the limited space, this research did not discuss the specific methods. The authors suggest that future research should explore which methods operate better than CFI when the required displaced left-turn lane is long. (3) The effects of non-motorized vehicles and pedestrians on the operational performance of CFI were not considered in this research. In addition, the traffic organization of CFI is significantly different from that of conventional intersections, and the authors suggest to study the traffic organization of non-motorized vehicles and pedestrians at CFI and explore its influence on CFI performance in future research.

Author Contributions: Conceptualization, B.P. and S.L. (Shasha Luo); methodology, B.P., S.L. (Shasha Luo) and Y.S.; data collection, S.L. (Shasha Luo), J.Y., S.L. (Shangru Liu) and J.L.; formal analysis, B.P., S.L. (Shasha Luo) and J.Y.; VISSIM simulation, X.L., J.L. and S.L. (Shasha Luo); visualization, B.P., S.L. (Shasha Luo), Y.S. and X.L.; writing—review and editing, B.P. and S.L. (Shasha Luo). All authors have read and agreed to the published version of the manuscript.

Funding: This work was supported by the China Scholarship Council with file No. 201506560015.

Data Availability Statement: The DOI for the data is 10.6084/m9.figshare.14807862 (accessed on accessed on 8 May 2021).

Acknowledgments: The authors would like to acknowledge the China Scholarship Council for partially funding this work.

Conflicts of Interest: The authors declare no conflict of interest.

References

1. Fang, S.; Zhao, C.; Hu, J.; Xing, Y.; Meng, Q.; Yu, X.; Wang, H.; Wang, P.; Zhang, R.; Gao, P. Temporal variations of pm2.5-bound platinum group elements in outdoor and indoor environments close to areas with traffic congestion. *Atmos. Environ.* **2021**, *246*, 118109. [CrossRef]
2. Pi, M.; Yeon, H.; Son, H.; Jang, Y. Visual cause analytics for traffic congestion. *IEEE Trans. Vis. Comput. Graph.* **2019**, *14*, 1. [CrossRef]
3. Zhao, J.; Gao, X.; Victor, L.K. An innovative design for left turn bicycles at continuous flow intersections. *Transp. Transp. Dyn.* **2019**, *7*, 1305–1322.
4. Bagloee, S.; Asadi, M. Crash analysis at intersections in the CBD: A survival analysis model. *Transp. Res. Part Policy Pract.* **2016**, *94*, 558–572. [CrossRef]
5. Mirheli, A.; Hajibabai, L.; Hajbabaie, A. Development of a Signal-head-free Intersection Control Logic in a Fully Connected and Autonomous Vehicle Environment. *Transp. Res. Part Emerg. Technol.* **2018**, *92*, 412–425. [CrossRef]
6. Tong, Y.; Zhao, L.; Li, L.; Zhang, Y. Stochastic programming model for oversaturated intersection signal timing. *Transp. Res. Part Emerg. Technol.* **2015**, *58*, 474–486. [CrossRef]
7. Yang, S.; Yang, B. A semi-decentralized feudal multi-agent learned-goal algorithm for multi-intersection traffic signal control. *Knowl.-Based Syst.* **2021**, *213*, 106708. [CrossRef]

8. Xu, H.; Zhuo, Z.; Chen, J.; Fang, X. Traffic signal coordination control along oversaturated two-way arterials. *Peerj Comput. Sci.* **2020**, *6*, e319. [CrossRef]
9. Yao, R.; Zhang, W.; Long, M.; Pekař, L. Comparative Analysis of Optimization Models for Paired Intersections with Left-Turn Bays. *Math. Probl. Eng.* **2020**, *2020*, 1–15. [CrossRef]
10. Qadri, S.S.S.M.; Gökçe, M.A.; Öner, E. State-of-art review of traffic signal control methods: Challenges and opportunities. *Eur. Transp. Res. Rev.* **2020**, *12*, 1–23. [CrossRef]
11. Yang, Z.; Liu, P.; Tian, Z.; Wang, W. Effects of Left-Turn Waiting Areas on Capacity and Level of Service of Signalized Intersections. *J. Transp. Eng.* **2013**, *139*, 1076–1085. [CrossRef]
12. Yang, Z.; Liu, P.; Tian, Z.; Wang, W. Evaluating the Operational Impact of Left-Turn Waiting Areas at Signalized Intersections in China. *Transp. Res. Rec. J. Transp. Res. Board* **2012**, *2286*, 12–20. [CrossRef]
13. Ma, W.; Liu, Y.; Zhao, J.; Wu, N. Increasing the capacity of signalized intersections with left-turn waiting areas. *Transp. Res. Part Policy Pract.* **2017**, *105*, 181–196. [CrossRef]
14. Dong, S; Yang, Z.; Xu, C.; Tian, Z.; Liu, P. Multiobjective Evaluation of Left-Turn Waiting Areas at Signalized Intersections in China. *Transp. Res. Rec. J. Transp. Res. Board* **2016**, *2553*, 138–149. [CrossRef]
15. Zhou, Y.; Zhuang, H. Traffic Performance in Signalized Intersection with Shared Lane and Left-Turn Waiting Area Established. *J. Transp. Eng.* **2012**, *138*, 852–862. [CrossRef]
16. DePrator, A.J.; Hitchcock, O.; Gayah, V.V. Improving Urban Street Network Efficiency by Prohibiting Conflicting Left Turns at Signalized Intersections. *Transp. Res. Rec. J. Transp. Res. Board* **2017**, *2622*, 58–69. [CrossRef]
17. Zhao, J.; Liu, Y.; Li, P. A network enhancement model with integrated lane reorganization and traffic control strategies. *J. Adv. Transp.* **2016**, *50*, 1090–1110. [CrossRef]
18. Shao, Y.; Han, X.; Wu, H.; Claudel, C.G. Evaluating Signalization and Channelization Selections at Intersections Based on an Entropy Method. *Entropy* **2019**, *21*, 808. [CrossRef]
19. Shao, Y.; Yu, H.; Wu, H.; Han, X.; Zhou, X.; Claudel, C.G.; Zhang, H.; Yang, C. Evaluation of an Exclusive Spur Dike U-Turn Design with Radar-Collected Data and Simulation. *J. Vis. Exp. JOVE* **2020**, *156*, e60675. [CrossRef]
20. Wu, J.; Liu, P.; Zhou, Y.; Yu, H. Stationary condition based performance analysis of the contraflow left-turn lane design considering the influence of the upstream intersection. *Transp. Res. Part Emerg. Technol.* **2021**, *122*, 102919. [CrossRef]
21. Chen, X.; Jia, Y. Sustainable traffic management and control system for arterial with contraflow left-turn lanes. *J. Clean. Prod.* **2021**, *280*, 124256. [CrossRef]
22. Zheng, Y.; Hua, X.; Wang, W.; Xiao, J.; Li, D. Analysis of a Signalized Intersection with Dynamic Use of the Left-Turn Lane for Opposite through Traffic. *Sustainability* **2020**, *12*, 7530. [CrossRef]
23. Zhao, J.; Ma, W; Zhang, H.M.; Yang, X. Increasing the Capacity of Signalized Intersections with Dynamic Use of Exit Lanes for Left-Turn Traffic. *Transp. Res. Rec.* **2013**, *2355*, 49–59. [CrossRef]
24. Combinido, J.S.L.; Lim, M.T. Modeling U-turn traffic flow. *Physica A* **2010**, *389*, 3640–3647. [CrossRef]
25. Shao, Y.; Han, X.; Wu, H.; Shan, H.; Yang, S.; Claudel, C.G. Evaluating the sustainable traffic flow operational features of an exclusive spur dike U-turn lane design. *PLoS ONE* **2019**, *14*, e0214759. [CrossRef] [PubMed]
26. Dhatrak, A.; Edara, P.; Bared, J.G. Performance Analysis of Parallel Flow Intersection and Displaced Left-Turn Intersection Designs. *Transp. Res. Rec.* **2010**, *2171*, 33–43. [CrossRef]
27. Sayed, T.; Storer, P.; Wong, G. Upstream Signalized Crossover Intersection: Optimization and Performance Issues. *Transp. Res. Rec.* **2006**, *1961*, 44–54. [CrossRef]
28. Tollazzi, T.; Tesoriere, G.; Guerrieri, M.; Campisi, T. Environmental, functional and economic criteria for comparing "target roundabouts" with one-or two-level roundabout intersections. *Transp. Res. Part D* **2015**, *34*, 330–344. [CrossRef]
29. Guerrieri, M.; Corriere, F.; Parla, G.; Vincenzo, D.D.; Messineo, A. Reducing Air Pollutants through Road Innovative Intersections. *Appl. Mech. Mater.* **2014**, *2828*, 563–568. [CrossRef]
30. Zhao, J.; Liu, Y.; Wang, T. Increasing Signalized Intersection Capacity with Unconventional Use of Special Width Approach Lanes. *Comput.-Aided Civ. Infrastruct. Eng.* **2016**, *31*, 794–810. [CrossRef]
31. You, X.; Li, L.; Ma, W. Coordinated Optimization Model for Signal Timings of Full Continuous Flow Intersections. *Transp. Res. Rec.* **2013**, *2366*, 23–33. [CrossRef]
32. Yang, X.; Chang, G.; Rahwanji, S.; Lu, Y. Development of Planning-Stage Models for Analyzing Continuous Flow Intersections. *J. Transp. Eng.* **2013**, *139*, 1124–1132. [CrossRef]
33. Liu, Q.; Zhang, L.; Yang, W. A New Continuous Flow Intersection for Urban Road: Architecture, Design, and Simulation. *Appl. Mech. Mater.* **2012**, *1976*, 677–682. [CrossRef]
34. Jiang, X.; Gao, S. Signal control method and performance evaluation of an improved displaced left-turn intersection design in unsaturated traffic conditions. *Transp. Transp. Dyn.* **2020**, *8*, 264–289. [CrossRef]
35. Zhao, J.; Ma, W; Head, K.L.; Yang, X. Optimal operation of displaced left-turn intersections: A lane-based approach. *Transp. Res. Part Emerg. Technol.* **2015**, *61*, 29–48. [CrossRef]
36. Tanwanichkul, L.; Pitaksringkarn, J.; Boonchawee, S. Determining the Optimum Distance of Continuous Flow Intersection Using Traffic Micro-simulation. *J. East. Asia Soc. Transp. Stud.* **2011**, *9*, 1670–1683.
37. Carroll, D.H.; Lahusen, D. Operational Effects of Continuous Flow Intersection Geometrics: A deterministic Model. *Transp. Res. Rec.* **2013**, *2348*, 1–11. [CrossRef]

38. Federal Highway Administration. Displaced Left Turn Intersection: Informational Guide. 2014. Available online: https://rosap.ntl.bts.gov/view/dot/29475 (accessed on 17 April 2021)
39. Jagannathan, R.; Bared, J.G. Design and Performance Analysis of Pedestrian Crossing Facilities for Continuous Flow Intersections. *Transp. Res. Rec.* **2005**, *1939*, 133–144. [CrossRef]
40. Sun, W.; Wu, X.; Wang, Y.; Yu, G. A continuous-flow-intersection-lite design and traffic control for oversaturated bottleneck intersections. *Transp. Res. Part Emerg. Technol.* **2015**, *56*, 18–33. [CrossRef]
41. Coates, A.; Yi, P.; Liu, P.; Ma, X. Geometric and Operational Improvements at Continuous Flow Intersections to Enhance Pedestrian Safety. *Transp. Res. Rec.* **2014**, *2436*, 60–69. [CrossRef]
42. Yang, X.; Cheng, Y. Development of signal optimization models for asymmetric two-leg continuous flow intersections. *Transp. Res. Part Emerg. Technol.* **2017**, *74*, 306–326. [CrossRef]
43. Suh, W.; Hunter, M.P. Signal design for displaced left-turn intersection using Monte Carlo method. *KSCE J. Civ. Eng.* **2014**, *18*, 1140–1149. [CrossRef]
44. Yang, X.; Cheng, Y.; Chang, G. Operational Analysis and Signal Design for Asymmetric Two-Leg Continuous-Flow Intersection. *Transp. Res. Rec. J. Transp. Res. Board* **2016**, *2553*, 72–81. [CrossRef]
45. Shams, A.; Zlatkovic, M. Effects of capacity and transit improvements on traffic and transit operations. *Transp. Plan. Technol.* **2020**, *43*, 602–619. [CrossRef]
46. Jagannathan, R.; Bared, J.G. Design and Operational Performance of Crossover Displaced Left-Turn Intersections. *Transp. Res. Rec. Transp. Res. Rec.* **2004**, *1881*, 1–10. [CrossRef]
47. Reid, J.D.; Hummer, J.E. Travel Time Comparisons Between Seven Unconventional Arterial Intersection Designs. *Transp. Res. Rec. J. Transp. Res. Board* **2001**, *1751*, 56–66. [CrossRef]
48. Autey, J.; Sayed, T.; Esawey, M.E. Operational performance comparison of four unconventional intersection designs using micro-simulation. *J. Adv. Transp.* **2013**, *47*, 536–552. [CrossRef]
49. Inman, V.W. Evaluation of Signs and Markings for Partial Continuous Flow Intersection. *Transp. Res. Rec. J. Transp. Res. Board* **2009**, *2138*, 66–74. [CrossRef]
50. Qu, W.; Sun, Q.; Zhao, Q.; Tao, T.; Qi, Y. Statistical Analysis of Safety Performance of Displaced Left-Turn Intersections: Case Studies in San Marcos, Texas. *Int. J. Environ. Res. Public Health* **2020**, *17*, 6446–6446. [CrossRef]
51. AutoNavi Traffic Big-Data. *Traffic Analysis Reports for Major Cities in China*; 2020. Available online: https://report.amap.com/share.do?id=a187b9ae753f219a01755470efdc6127 (accessed on 23 October 2020).
52. Chen, H.; Zhang, N.; Qian, Z. VISSIM-Based Simulation of the Left-Turn Waiting Zone at Signalized Intersection. In Proceedings of the 2008 International Conference on Intelligent Computation Technology and Automation (ICICTA), Changsha, China, 20–22 October 2008; pp. 736–740.
53. Federal Highway Administration (FHWA). *Surrogate Safety Assessment Model (SSAM)—SOFTWARE USER MANUAL*; Federal Highway Administration: Washiton, DC, USA, 2008.
54. Ran, B.; Song, L.; Zhang, J.; Cheng, Y.; Tan, H. Using Tensor Completion Method to Achieving Better Cover-age of Traffic State Estimation from Sparse Floating Car Data. *PLoS ONE* **2016**, *11*, e0157420. [CrossRef]
55. Zhao, J.; Li, P.; Zhou, X. Capacity Estimation Model for Signalized Intersections under the Impact of Access Point. *PLoS ONE* **2016**, *11*, e0145989. [CrossRef]
56. Henclewood, D.; Suh, W.; Rodgers, M.O.; Fujimoto, R.; Hunter, M.P. A calibration procedure for increasing the accuracy of microscopic traffic simulation models. *SIMULATION* **2017**, *93*, 35–47. [CrossRef]
57. Xiang, Y.; Li, Z.; Wang, W.; Chen, J.; Wang, H.; Li, Y. Evaluating the Operational Features of an Unconventional Dual-Bay U-Turn Design for Intersections. *PLoS ONE* **2016**, *11*, e0158914. [CrossRef] [PubMed]
58. Wang, J.Y.; Mao, Y.; Li, J.; Xiong, Z.; Wang, W.X. Predictability of Road Traffic and Congestion in Urban Areas. *PLoS ONE* **2015**, *10*, e0121825. [CrossRef] [PubMed]
59. Chang, A.S.; Tsai, C.Y. Difficulty and reasons for sustainable roadway design-the case from Taiwan. *J. Civ. Eng. Manag.* **2015**, *21*, 395–406. [CrossRef]
60. Chang, A.S.; Tsai, C.Y. Sustainable design indicators: Roadway project as an example. *Ecol. Indic.* **2015**, *53*, 137–143. [CrossRef]
61. Campisi, T.; Mrak, I.; Antonino, C.; Tesoriere, G. The surrogate safety measures evaluation of a staggered crossing on the delta area of Rijeka. *Aip Conf. Proc.* **2019**, *2186*, 160006.
62. Tesoriere, G.; Campisi, T.; Canale, A.; Zgrablić, T. The Surrogate Safety Appraisal of the Unconventional Elliptical and Turbo Roundabouts. *J. Adv. Transp.* **2018**, *2018*, 2952074. [CrossRef]
63. Federal Highway Administration Research and Technology. Surrogate Safety Assessment Model (SSAM) Publications. 2018. Available online: https://www.fhwa.dot.gov/publications/lists/020.cfm (accessed on 16 April 2021)
64. Haghshenas, H.; Vaziri, M. Urban sustainable transportation indicators for global comparison. *Ecol. Indic.* **2012**, *15*, 115–121. [CrossRef]
65. Chen, T.; Chen C.; Chuang, Y.; Liou J.J.H. A Hybrid MADM Model for Product Design Evaluation and Improvement. *Sustainability* **2020**, *12*, 6743–6743. [CrossRef]
66. Zhang, C.; Hu, Q.; Zeng, S.; Su, W. IOWLAD-based MCDM model for the site assessment of a household waste processing plant under a Pythagorean fuzzy environment. *Environ. Impact Assess. Rev.* **2021**, *89*, 106579. [CrossRef]

67. Per-Olof, P. A sparse and high-order accurate line-based discontinuous Galerkin method for unstructured meshes. *J. Comput. Phys.* **2013**, *233*, 414–429.
68. Tian, Z.P.; Wang, J.Q.; Zhang, H.Y. An integrated approach for failure mode and effects analysis based on fuzzy best-worst, relative entropy, and VIKOR methods. *Appl. Soft Comput.* **2018**, *72*, 636–646. [CrossRef]
69. Chen, W.; Li, H.; Wang, S.Q.; Wang, G.R.; Panahi, M.; Li, T.; Peng, T.; Guo, C.; Niu, C.; Xiao, L.; et al. GIS-based groundwater potential analysis using novel ensemble weights-of-evidence with logistic regression and functional tree models. *Sci. Total. Environ.* **2018**, *634*, 853–867. [CrossRef]
70. Shang, H.; Li, F.; Wu, Y. Partial Discharge Fault Diagnosis Based on Multi-Scale Dispersion Entropy and a Hypersphere Multiclass Support Vector Machine. *Entropy* **2019**, *21*, 81. [CrossRef]
71. Zhao, X.; Liang, C.; Zhang, N.; Shang, P. Quantifying the Multiscale Predictability of Financial Time Series by an Information-Theoretic Approach. *Entropy* **2019**, *21*, 684. [CrossRef] [PubMed]
72. American Association of State and Highway Transportation Officials (AASHTO). *A Policy on Geometric Design of Highways and Streets*, 7th ed.; AASHTO: Washington, DC, USA, 2018.
73. Jian, S. *Guideline for Microscopic Traffic Simulation Analysis*; Tongji University Press: Shanghai, China, 2014.
74. Transportation Research Board (TRB). *Highway Capacity Manual*, 6th ed.; A Guide for Multimodal Mobility Analysis (HCM): Washington, DC, USA, 2016.